

## Supporting Information

**Aligned Networks of Engineered Fibrillar Fibronectin Guide Cellular Orientation and Motility**

*Dylan B. Neale, Ayşe J. Muñiz, Michael S. Jones, Do Hoon Kim, Johanna M. Buschhaus, Brock A. Humphries, William Y. Wang, Brendon M. Baker, Jeffery E. Raymond, Luis Solorio, Gary D. Luker, Joerg Lahann\**

1. *A brief discussion of the interpretation of FFT spectral analysis:*

The artificial bins represent intensity residuals when features in the more aligned (closer to 0 degree) and less aligned (closer to  $\pm 90^\circ$ ) are removed. As an example: a bin at  $18^\circ$  ( $16^\circ - 20^\circ$  binning) is the difference between the intensity of 0 to  $+20^\circ$  and 0 to  $+16^\circ$ . The intensity of the spectra in each of these bins is an assessment of the intensity of feature alignment that gets redirected off axis, and not a direct count of parallel and perpendicular features. Therefore, the data is more analogous to elastic scattering techniques (x-ray; electron) than a true count-based analysis. The spectra from  $+90$  to  $-90^\circ$  is half of the spectra that could be obtained, where the second half of the spectra is merely a reflection of the first half; therefore, only  $+90^\circ$  to  $-90^\circ$  spectra are reported.

2. *A brief discussion of the alignment parameter:*

The alignment parameter (*AP*) is defined as the area under the Gaussian curve, normalized by the area under the y-offset, see **Figure S9** for a graphical representation.

$$\text{Equation 1: } AP = \frac{a_{aligned}}{a_{non-aligned}}$$

Perfectly aligned fibrils would be a narrow distribution with no y-offset, and completely random fibrils would be flat distribution with no curve. Both the full width at half maximum (FWHM) and *AP* are considered in describing the characteristics of the data.

3. *Equations used in assessing motility data:*

The diffusivity in either direction is calculated from the speed (*S*) and persistence time (*P*), Equation 2.

$$\text{Equation 2: } D = \frac{S^2 P}{4}$$

The anisotropic index ( $\phi$ ) is the diffusivity (*D*) along the primary (*p*) axis divided by diffusivity along the non-primary (*np*) axis, Equation 3.

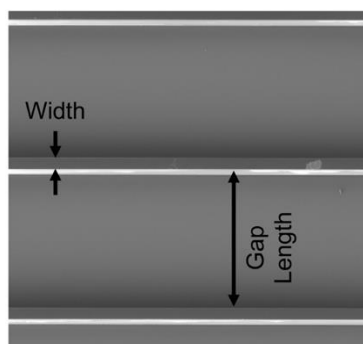
$$\text{Equation 3: } \phi = \frac{D_p}{D_{np}} = \frac{S_p^2 P_p}{S_{np}^2 P_{np}}$$

#### 4. A brief discussion of fluid flow rates:

8 RPM was found through qualitative inspection of the 2D COMSOL model to produce fluid flows of  $\sim 0.15\text{m/s}$  (**Figure S2, S3**). This value was employed as the inlet velocity of the 3D model. At this flow rate, fluid flow streamlines were found to be coherently aligned across the length of the tessellated polymer scaffold (TPS). At half of this rate ( $0.075\text{m/s}$ ) there was not a substantial improvement in fluid flow profiles, through qualitative inspection (**Figure S17**). Furthermore, at lower rotational velocities, the number of fluid-scaffold contacts would be decreased during the coating process. At higher flow rates ( $0.3\text{m/s}$ ) vortices are observed (**Figure S17**).

#### 5. Supplemental table describing SU-8 TPS dimensions:

**Supplemental Table 1.** Top: SEM of a SU-8 TPS. Reported in the table are target values versus measured. Measured values came from images taken in DPBS, representing the geometry *in situ* during the coating process. Height was measured using contact profilometry in a dry state. Data reported as average  $\pm$  standard deviation.



	Rectangle 245	Rectangle 500	Rectangle 950	SU-8 Spin Height
Gap Length Target ( $\mu\text{m}$ )	245	500	950	n/a
Gap Length Measured ( $\mu\text{m}$ )	$248 \pm 3.2$	$497 \pm 5.0$	$946 \pm 2.6$	n/a
Width Target ( $\mu\text{m}$ )	35	35	35	n/a
Width Measured ( $\mu\text{m}$ )	$35 \pm 1.2$	$36 \pm 0.7$	$35 \pm 1.6$	n/a
Approximate Free Volume (%)	88	94	97	n/a
Height Target ( $\mu\text{m}$ )				110
Height Measured ( $\mu\text{m}$ )				$112 \pm 1.7$

## 6. Fibronectin-based biomaterials

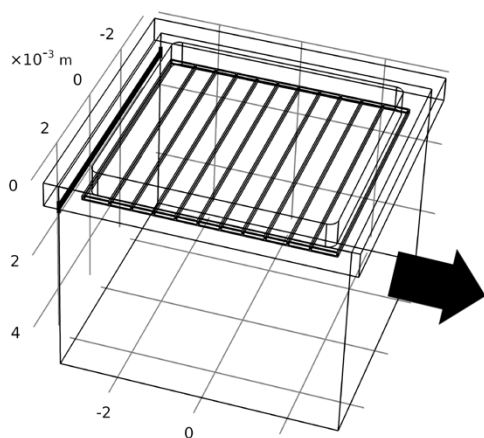
**Supplemental Table 2.** A summary of fibronectin-based biomaterials and their characteristics. Documented are the methods of Fn assembly, the ability to control orientation in order to create aligned or non-aligned matrices, the dimensionality (i.e. 2D/3D), overall x-y material scale, fiber diameters, their microstructure, and the type of substrate (i.e., free standing, suspended, or adhered to a surface/2D material). If a material is noted as 2.5D that indicates that the Fn network is relatively thin but are suspended or freestanding in such a way that differs from a conventional 2D substrate.

Method	Alignment (length scale)	Dimensionality	Overall area or length	Fiber diameter	Microstructure	Type of substrate	Ref.
solution		n.r.	cm <sup>2</sup>	10 ± 2.8 nm	n.r.	FS	[1,2]
shearing via impellers and syringes	yes, mm	3D	cm <sup>2</sup>	2-7 μm	Dense mats with tubular pores	FS	[3-5]
lipid monolayer expansion	no	n.r.	μm <sup>2</sup>	“few” μm	Fibrillar networks	n.r.	[6]
manually drawn from droplets	yes, mm	2D	mm	0.2-10 μm	Branched fibrillar networks	Adh.	[4,7]
manually drawn from droplets	yes, cm	1D	cm	2 - 5 μm	single fibers	Sus.	[8-10]
shearing across micropillars	yes, <10 μm gaps	2.5D	cm <sup>2</sup>	Single fibers: 20 - 160 nm fiber bundles: ~1-2 μm	Single fibers or fiber bundles bridging micropillars with <10 μm gaps	Sus.	[11,12]
rotary jet spinning	yes, <200 μm	3D	cm <sup>2</sup>	457 ± 138 nm	Fibrillar networks	FS	[13]
surface-induced	no	2D	cm <sup>2</sup>	≤10 μm	Fibrillar networks	Adh.	[14-16]
surface-induced	yes, mm	2.5D	mm <sup>2</sup>	3.7 ± 1.0 μm	User-defined patterns	Adh., Sus., FS	[17,18]

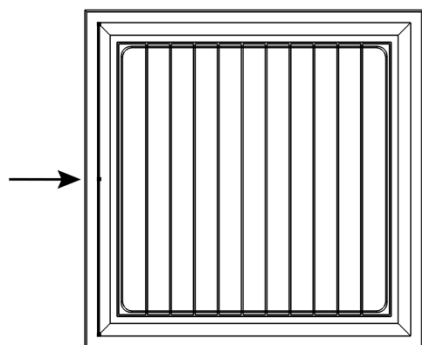
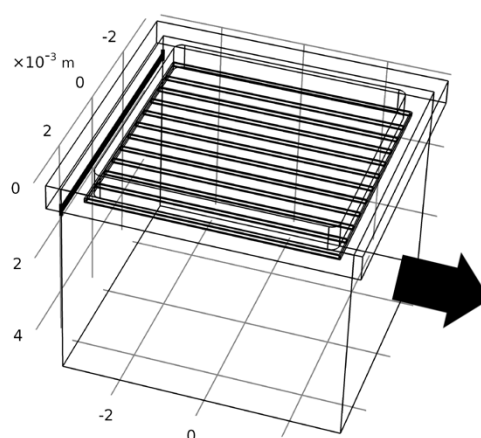
(Table acronyms/abbreviations: n.r. – not reported, FS – free standing; Sus. – suspended, Adh. – adhered to a 2D substrate; Ref. – references.)

## References

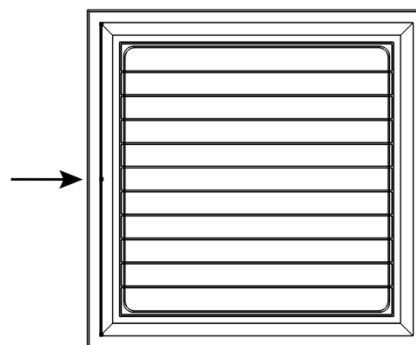
- [1] D. F. Mosher, R. B. Johnson, *J. Biol. Chem.* **1983**, 258, 6595.
- [2] Y. Chen, L. Zardi, D. M. P. Peters, *Scanning* **1997**, 19, 349.
- [3] Z. Ahmed, S. Underwood, R. A. Brown, *Tissue Eng.* **2003**, 9, 219.
- [4] O. S. Ejim, G. W. Blunn, R. A. Brown, *Biomaterials* **1993**, 14, 743.
- [5] S. Underwood, A. Afoke, R. A. Brown, A. J. MacLeod, P. A. Shamlou, P. Dunnill, *Biotechnol. Bioeng.* **2001**, 73, 295.
- [6] G. Baneyx, V. Vogel, *Proc. Natl. Acad. Sci.* **1999**, 96, 12518.
- [7] B. Wojciak-Stothard, M. Denyer, M. Mishra, R. A. Brown, *Vitr. Cell. Dev. Biol. - Anim.* **1997**, 33, 110.
- [8] W. C. Little, M. L. Smith, U. Ebnetter, V. Vogel, *Matrix Biol.* **2008**, 27, 451.
- [9] E. Klotzsch, M. L. Smith, K. E. Kubow, S. Muntwyler, W. C. Little, F. Beyeler, D. Gourdon, B. J. Nelson, V. Vogel, *Proc. Natl. Acad. Sci.* **2009**, 106, 18267.
- [10] M. Mitsi, S. Handschin, I. Gerber, R. Schwartländer, E. Klotzsch, R. Wepf, V. Vogel, *Biomaterials* **2015**, 36, 66.
- [11] J. Ulmer, B. Geiger, J. P. Spatz, *Soft Matter* **2008**, 4, 1998.
- [12] P. Kaiser, J. P. Spatz, *Soft Matter* **2010**, 6, 113.
- [13] C. O. Chantre, P. H. Campbell, H. M. Golecki, A. T. Buganza, A. K. Capulli, L. F. Deravi, S. Dauth, S. P. Sheehy, J. A. Paten, K. Gledhill, Y. S. Doucet, H. E. Abaci, S. Ahn, B. D. Pope, J. W. Ruberti, S. P. Hoerstrup, A. M. Christiano, K. K. Parker, *Biomaterials* **2018**, 166, 96.
- [14] J. Ballester-Beltrán, P. Rico, D. Moratal, W. Song, J. F. Mano, M. Salmerón-Sánchez, *Soft Matter* **2011**, 7, 10803.
- [15] N. Pernodet, M. Rafailovich, J. Sokolov, D. Xu, N.-L. Yang, K. McLeod, *J. Biomed. Mater. Res.* **2003**, 64A, 684.
- [16] P. Rico, J. C. R. Hernández, D. Moratal, G. Altankov, M. M. Pradas, M. Salmerón-Sánchez, *Tissue Eng. Part A* **2009**, 15, 3271.
- [17] A. W. Feinberg, K. K. Parker, *Nano Lett.* **2010**, 10, 2184.
- [18] S. Ahn, L. F. Deravi, S.-J. Park, B. E. Dabiri, J.-S. Kim, K. K. Parker, K. Shin, *Adv. Mater.* **2015**, 27, 2838.

**A****Perpendicular**

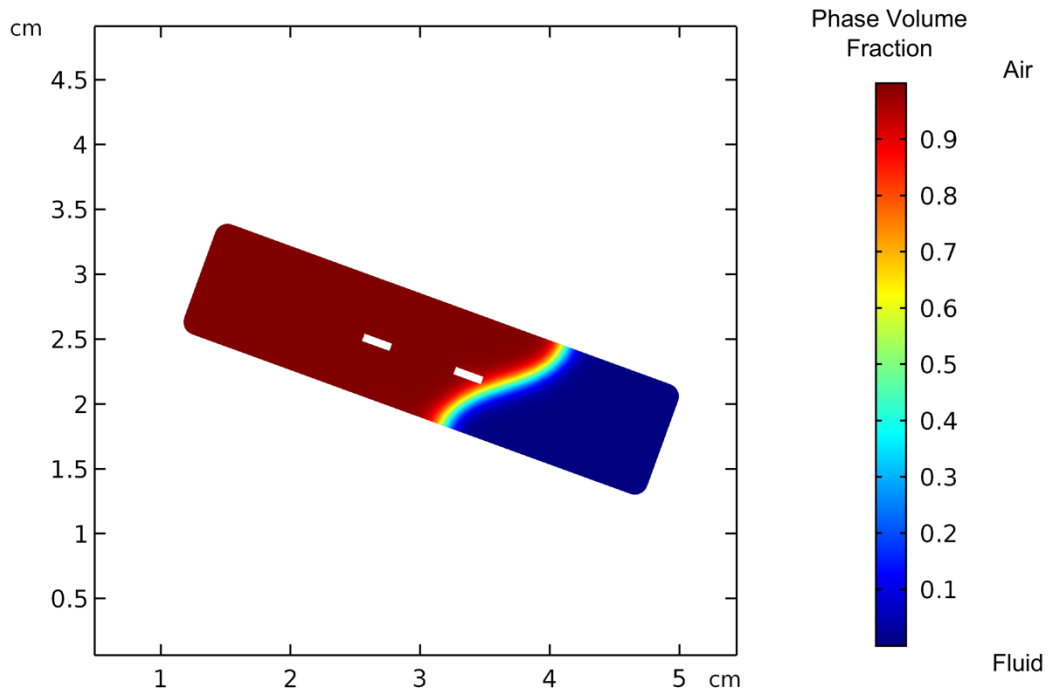
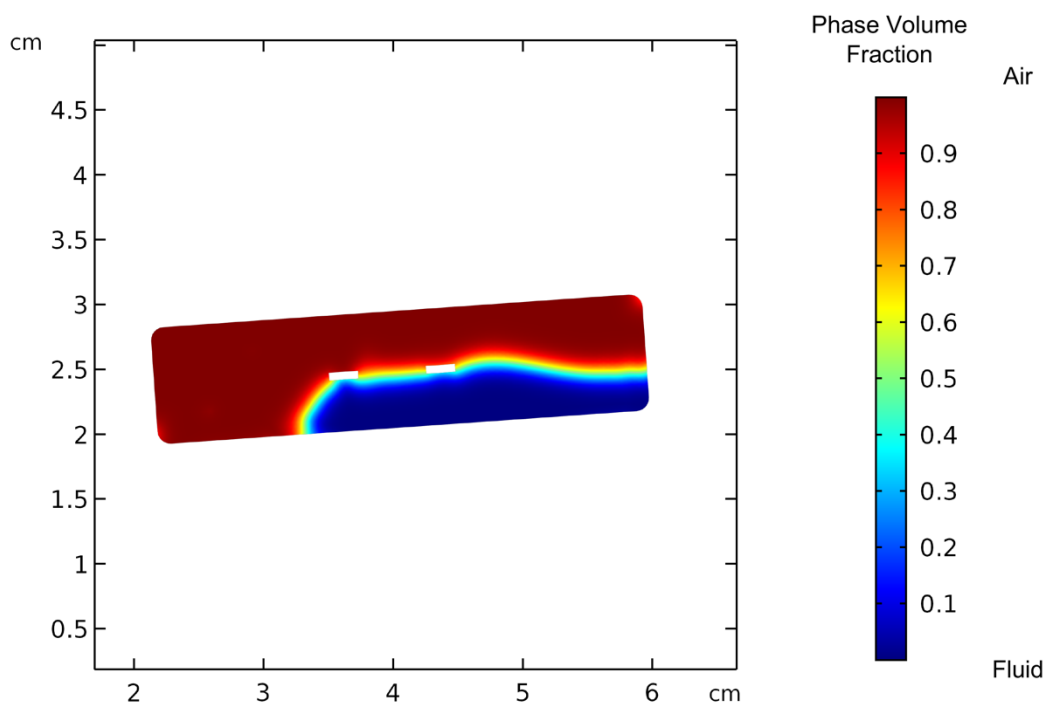
Top-down view

**B****Parallel**

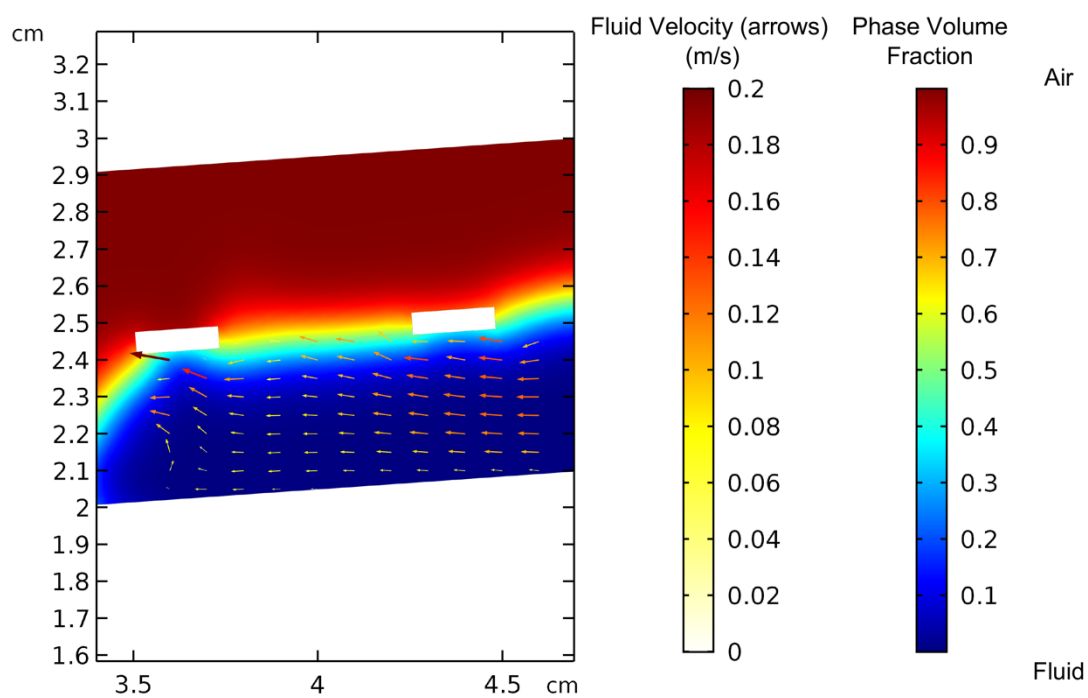
Top-down view



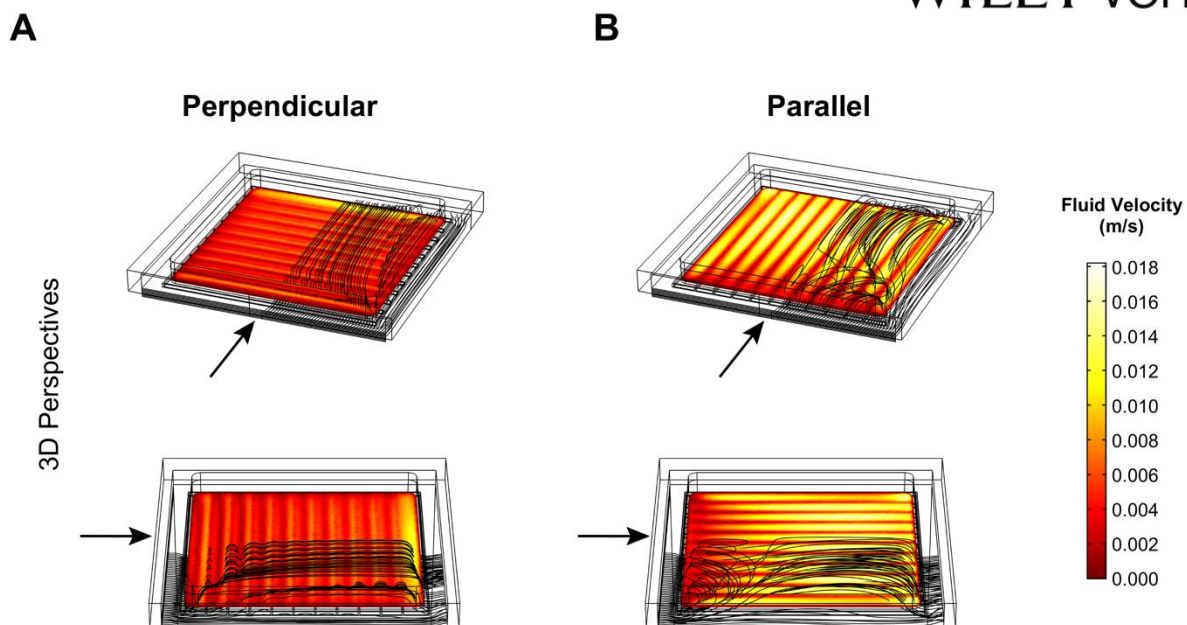
**Supplemental Figure 1.** Wireframe diagram of 3D COMSOL model. **A:** perpendicular orientation. **B:** parallel orientation. Grid marks are 2mm apart. The black arrows indicate fluid flow direction (large arrow – outlet, small arrow – inlet).

**A****B**

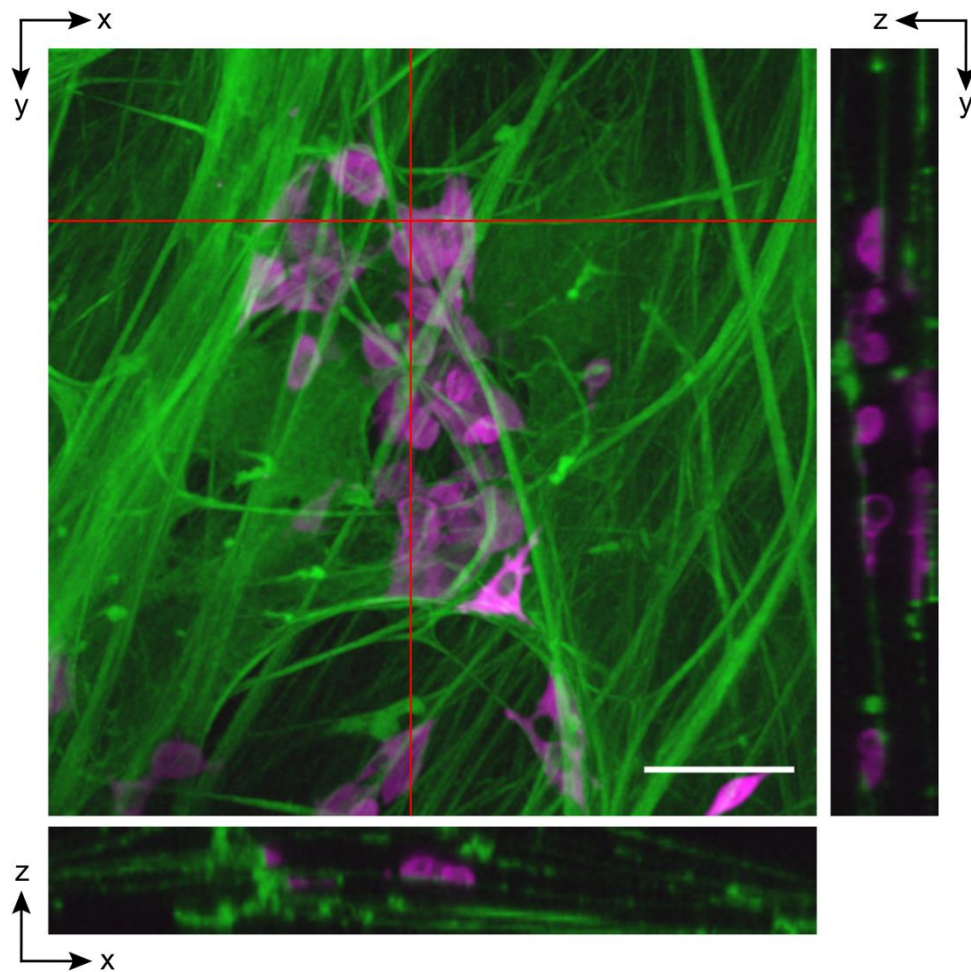
**Supplemental Figure 2:** two-phase, time dependent model used to assess the velocity of fluid during hydrodynamically-induced fibrillogenesis. **A:** at 1.45 s. **B:** 1.95 s. The white boxes represent the cross sections of the steel frames that were used to constrain the TPSs during the coating process. The two phases (fluid, air) are depicted with the blue to red scalar.



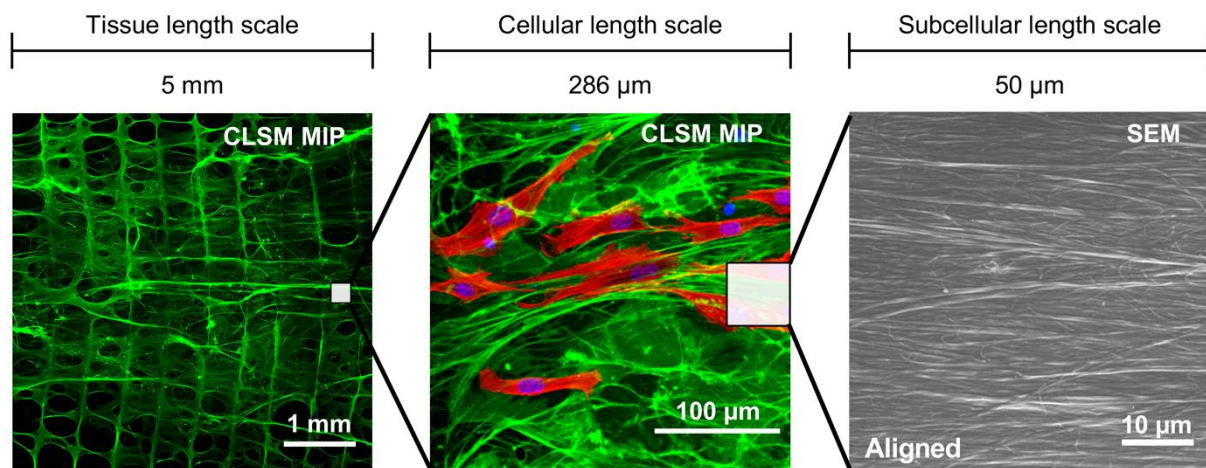
**Supplemental Figure 3.** Enlarged view of **Figure S2B** (1.45 s), which was used to evaluate the velocity of fluid flow during hydrodynamically-induced fibrillogenesis. Arrows and colors of the arrows (white to red scalar) indicate the direction of flow and velocity, respectively. The two phases (fluid, air) are depicted with the blue to red scalar.



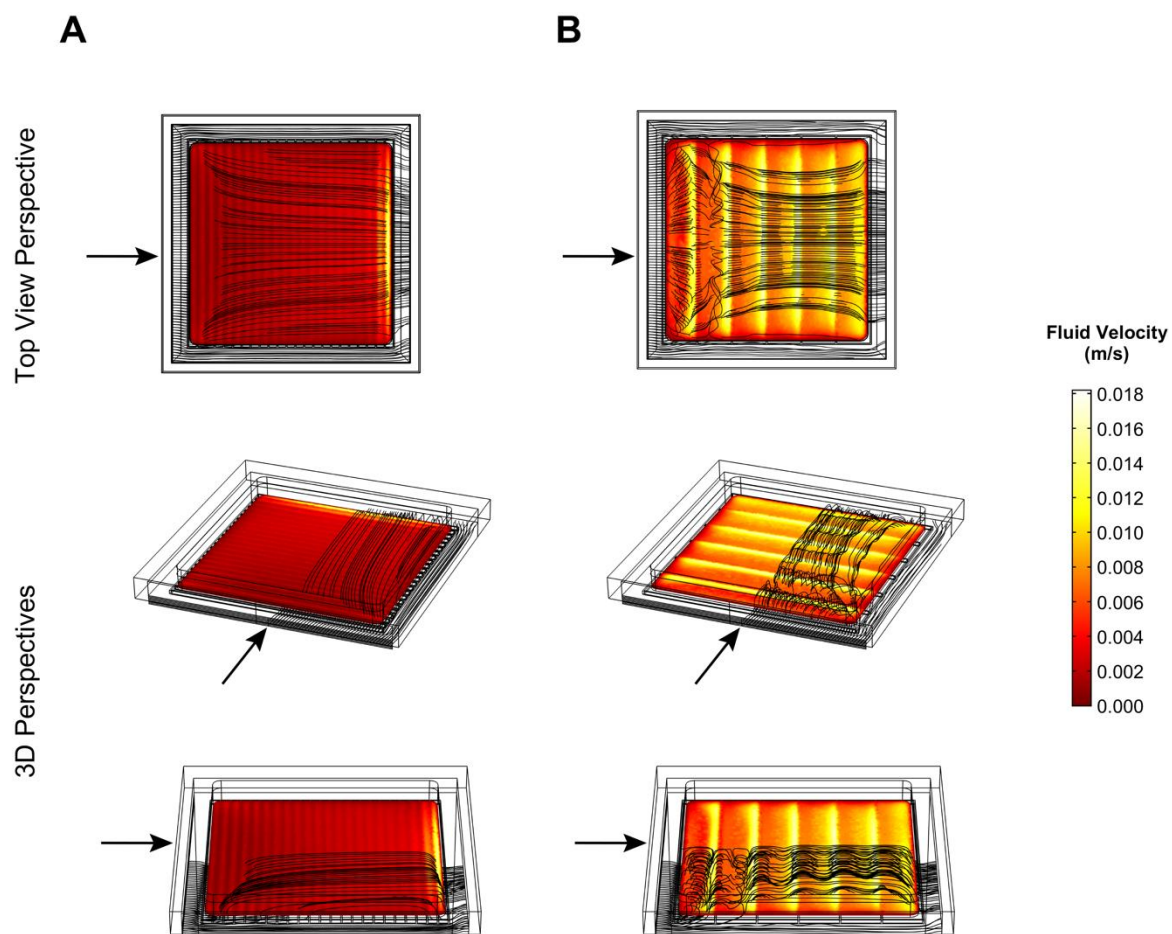
**Supplemental Figure 4.** 3D perspectives of the fluid flow profile across perpendicular (**A**) and parallel (**B**) oriented TPSs. Black arrows indicate fluid flow direction on the inlet side of the model. Streamlines are shown in black while velocities are represented by color.



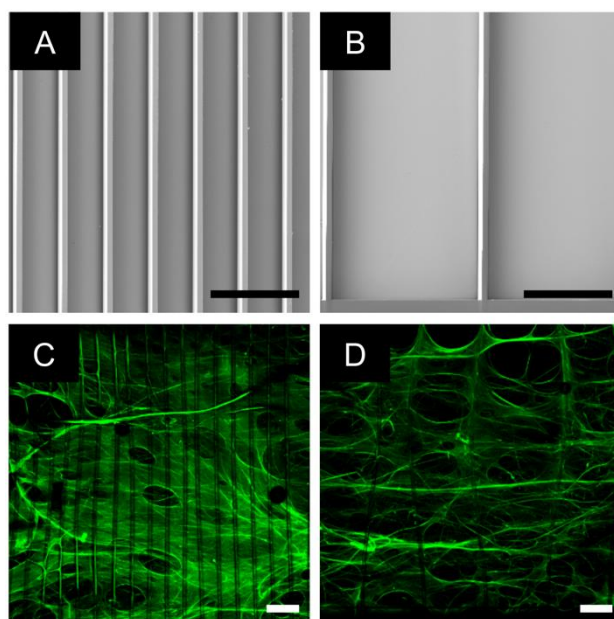
**Supplemental Figure 5** Image of MCF7 cells (magenta) cultured in an Fn EECM (green) demonstrates that cells integrate in the three-dimensional volume within EECMs. The center image is a 2-photon confocal MIP projected onto the xy plane. The right image is an yz orthogonal slice and the bottom image is an xz orthogonal slice. Slice locations are demonstrated with red lines. A Gaussian blur filter, sigma = 1.0, and gamma correction of 0.6 was applied to both channels for display purposes. Scale bar = 100  $\mu\text{m}$  and applies to all three views.



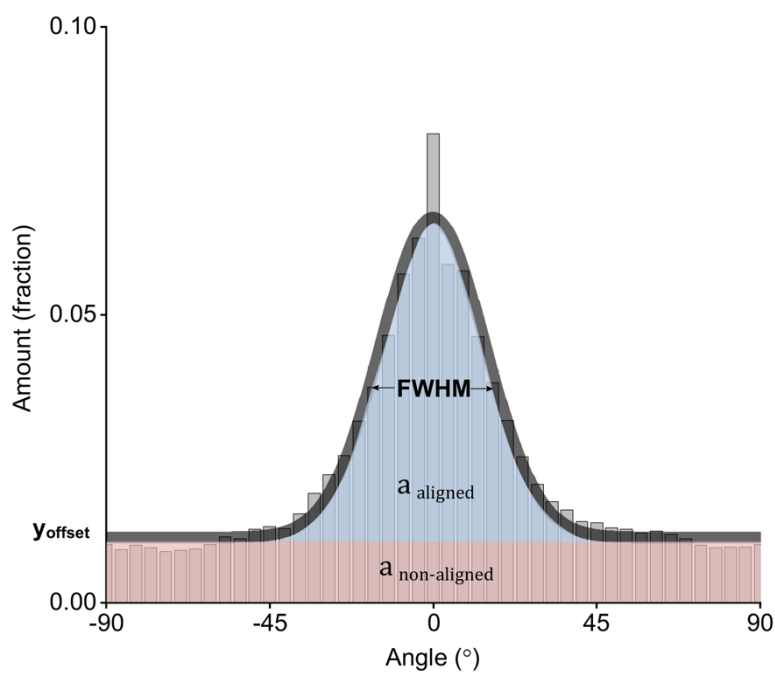
**Supplemental Figure 6.** Visual representation displaying the relative imaging length scales assessed throughout the manuscript. This demonstrates the achievement of fibril alignment from the multi-millimeter “tissue” length scale down to the submicron, “subcellular” length scale. Imaging studies performed at the “cellular” length scale is a scale in which multiple NIH-3T3 fibroblasts are captured within the same field of view. Approximate ROIs are shown on the tissue and cellular length scales in the white box. These images are not from the same sample but are compiled to illustrate relative scales.



**Supplemental Figure 7: Supplemental Figure 1.** 3D perspectives of the fluid flow profile across perpendicular oriented TPSs of 245  $\mu\text{m}$  (**A**) and 950  $\mu\text{m}$  gap lengths (**B**). Black arrows indicate fluid flow direction on the inlet side of the model. Streamlines are shown in black while velocities are represented by color.



**Supplemental Figure 8.** **A,C:** 250  $\mu\text{m}$  gap length TPSs. **B,D:** 950  $\mu\text{m}$  gap length TPSs. **A,B:** SEMs of the TPSs before coating. **C,D:** MIPs of the Fn networks after coating. Scale bars = 500  $\mu\text{m}$

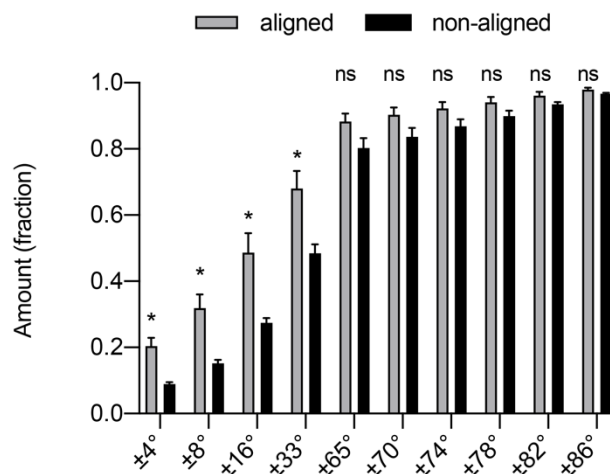


$$AP = \frac{a_{aligned}}{a_{non-aligned}}$$

**Supplemental Figure 9.** Visual representation of quantitative metrics used to describe directionality histograms. The full-width at half maximum (FWHM) is the width of the distribution at the y-value which is halfway from the baseline (y-offset) to the peak of the distribution. The alignment parameter (*AP*) describes a value where the area under the Gaussian (aligned features) is normalized by the area under the y-offset (non-aligned features).

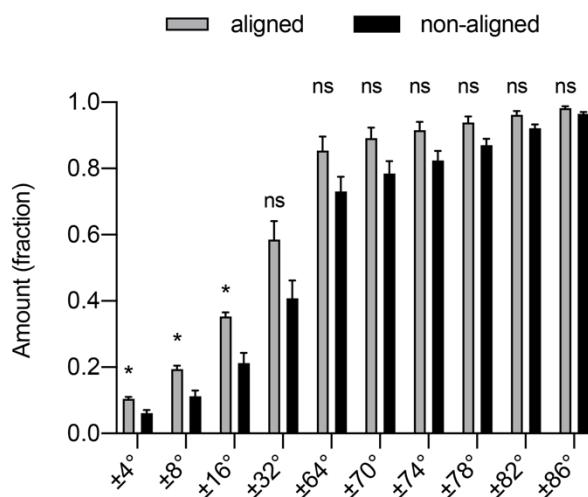
**A**

**Fibronectin directionality binning analysis**



**B**

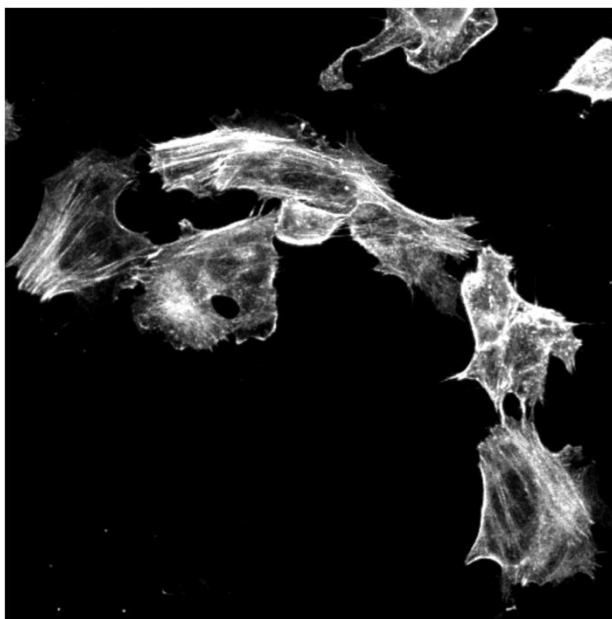
**Actin directionality binning analysis**



**Supplemental Figure 10. A:** Expanded directionality summation analysis of CLSM MIPs from **Figure 2E. B:** Expanded directionality binning analysis of CLSM MIPs from **Figure 3G.** The Holm-Sidak Multiple t-test was performed to compare groups and assess statistical significance. \* $P \leq 0.05$ , \*\* $P \leq 0.01$ , \*\*\* $P \leq 0.001$

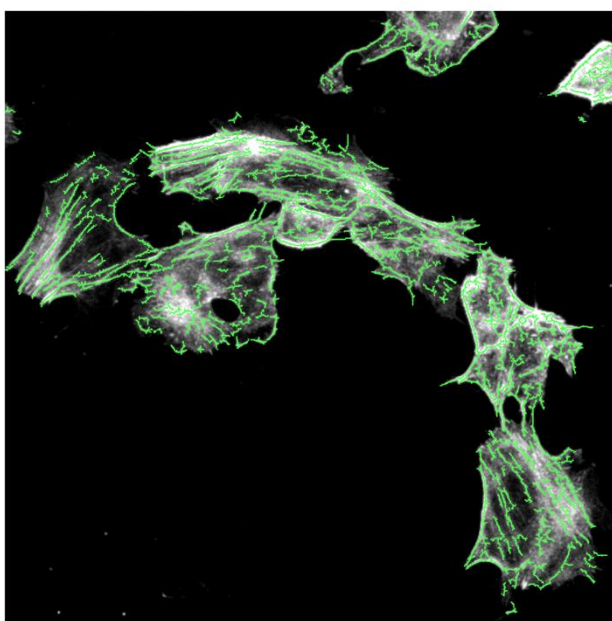
**A**

**F-actin stain**

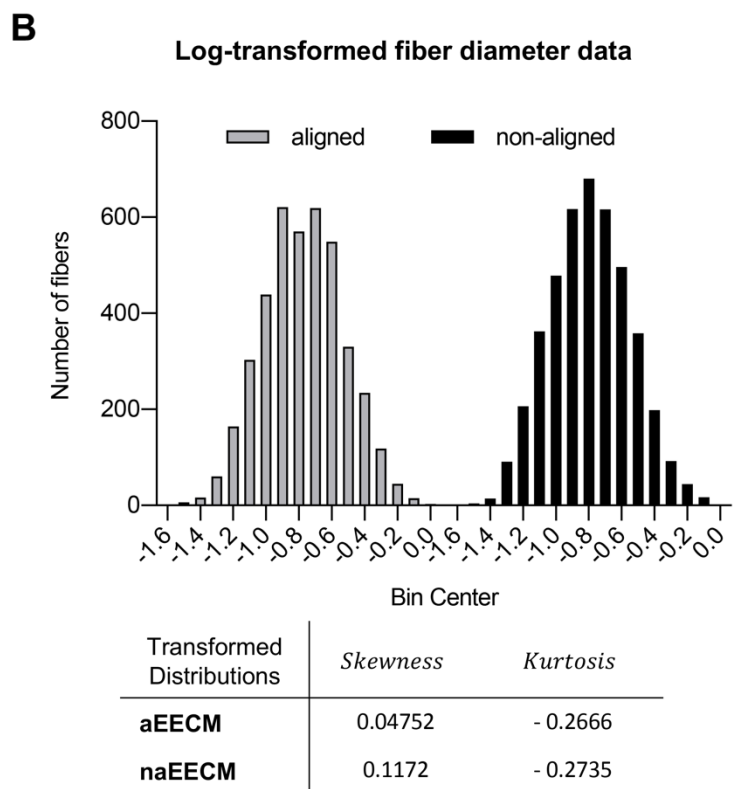
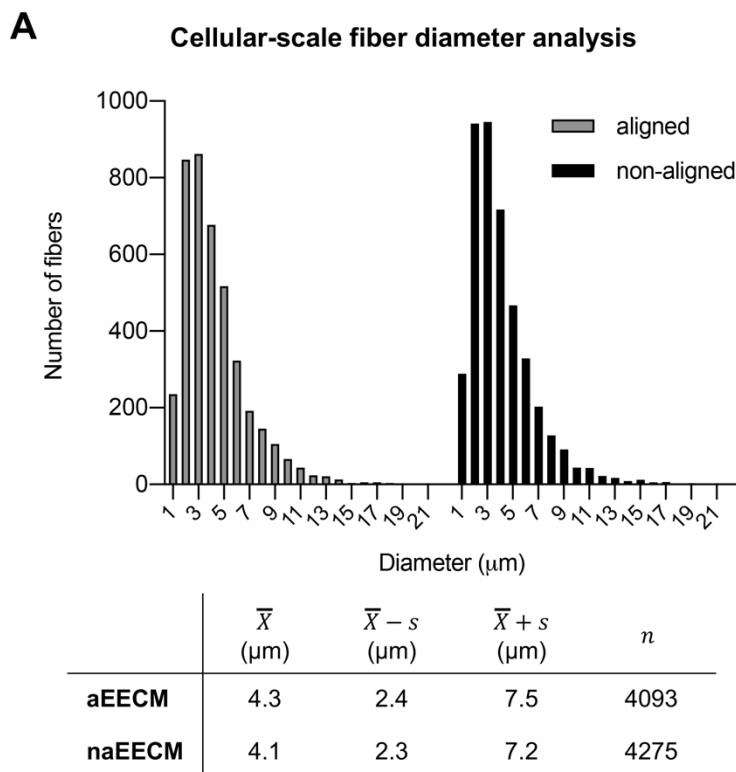


**B**

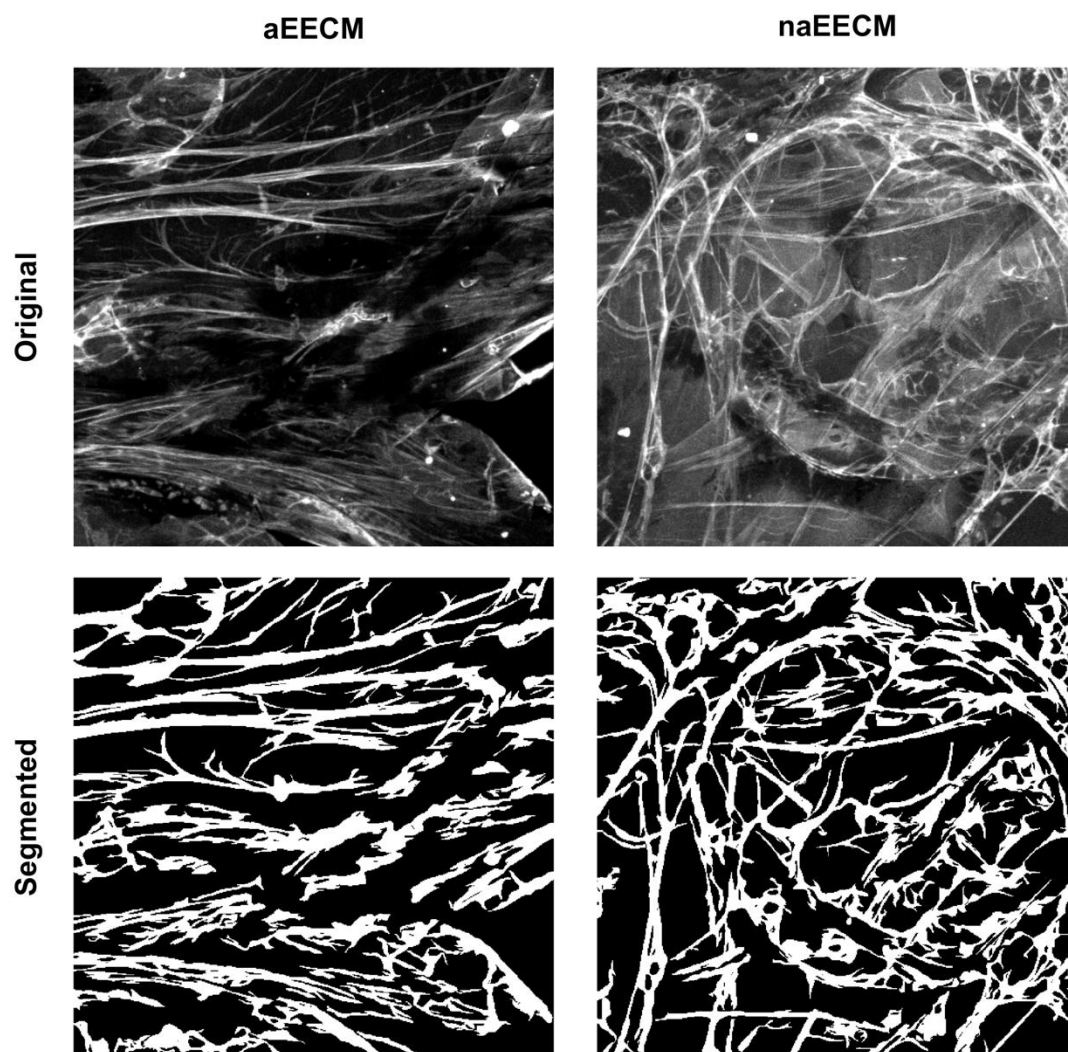
**Stress fiber analysis overlay**



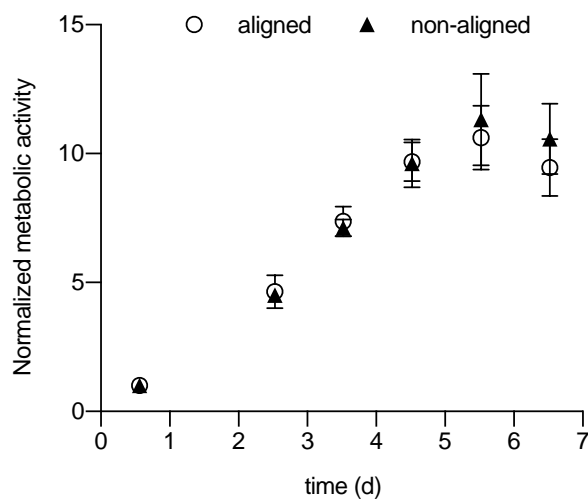
**Supplemental Figure 11.** Representative images from stress fiber analysis reported in **Figure 3H**.



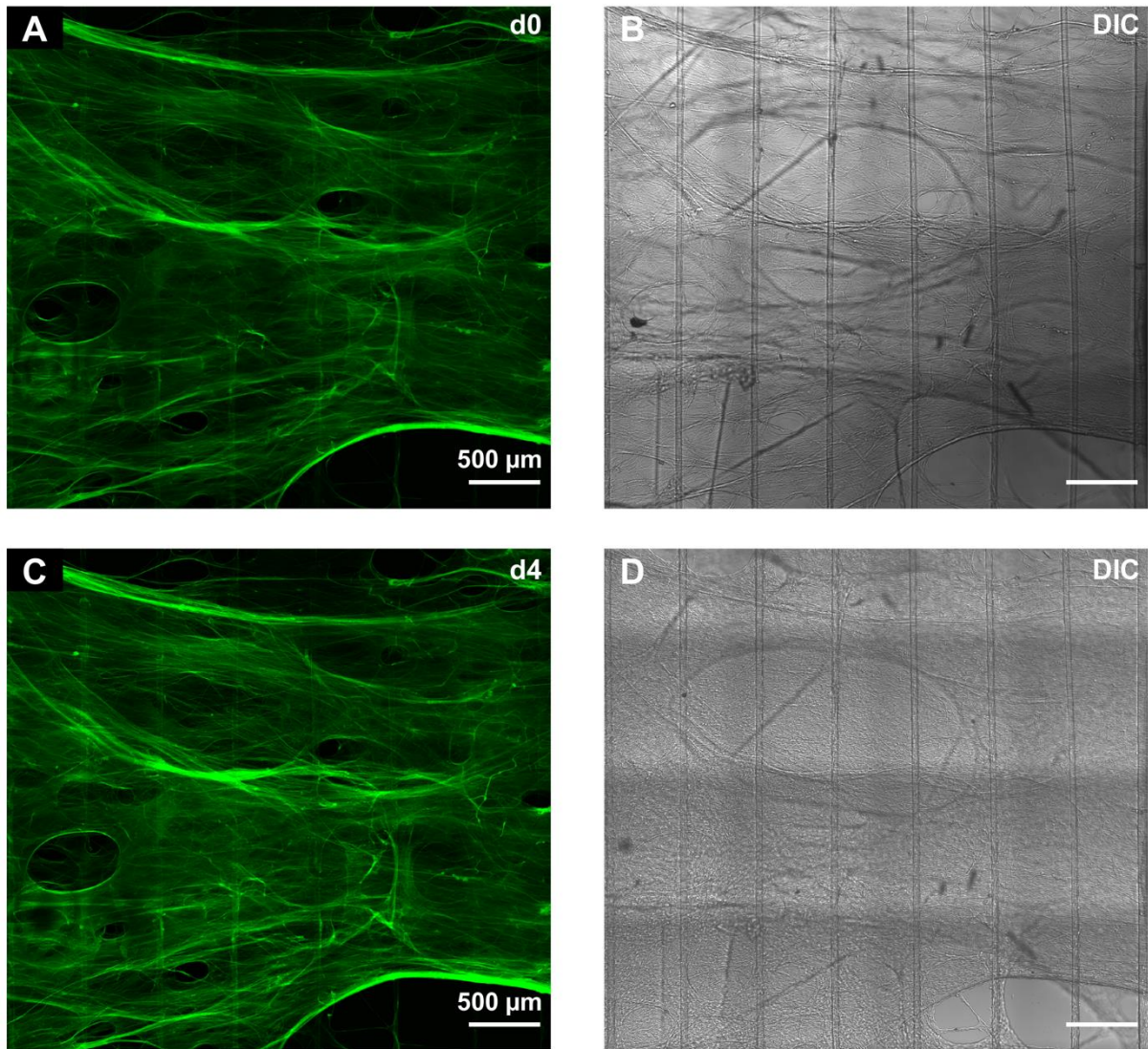
**Supplemental Figure 12:** **A:** Fn fibril diameter data generated from image analysis of CLSM MIPs of aEECM and naEECMs in **Figure 3**. Mean ( $\bar{X}$ ), mean  $\pm$  one sample standard deviation ( $\bar{X} \pm s$ ), and sample sizes ( $n$ ) are reported in the table below the graph. **B:** shows transformed diameter data, transformed *via* the equation:  $y' = \log_{10} \frac{y}{y_{max}}$ . Skewness and kurtosis are reported to indicate the data are sufficiently normal after transformation. Transformed data were used to generate the summary statistics reported in the table above.



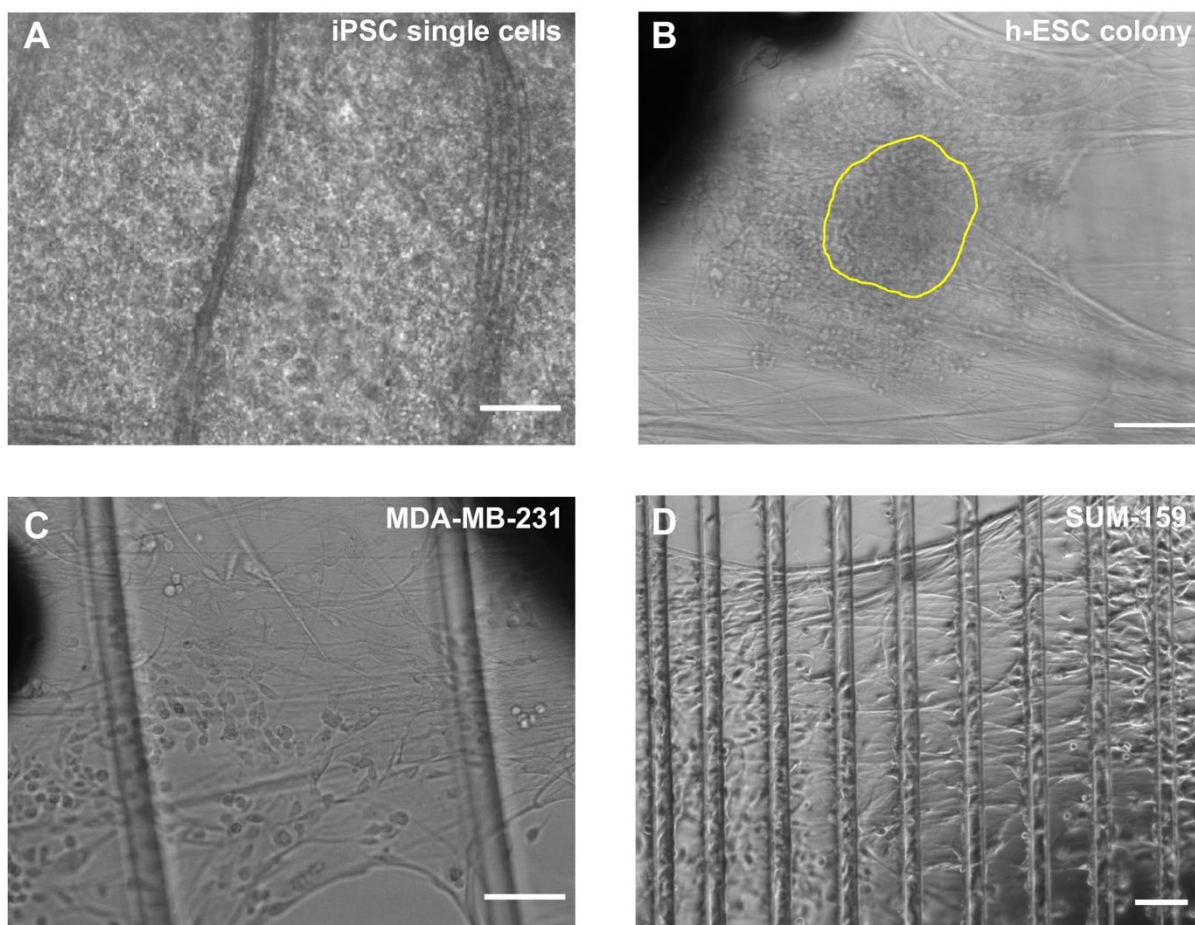
**Supplemental Figure 13.** Representative images from fiber diameter analysis reported in **Figure S12**



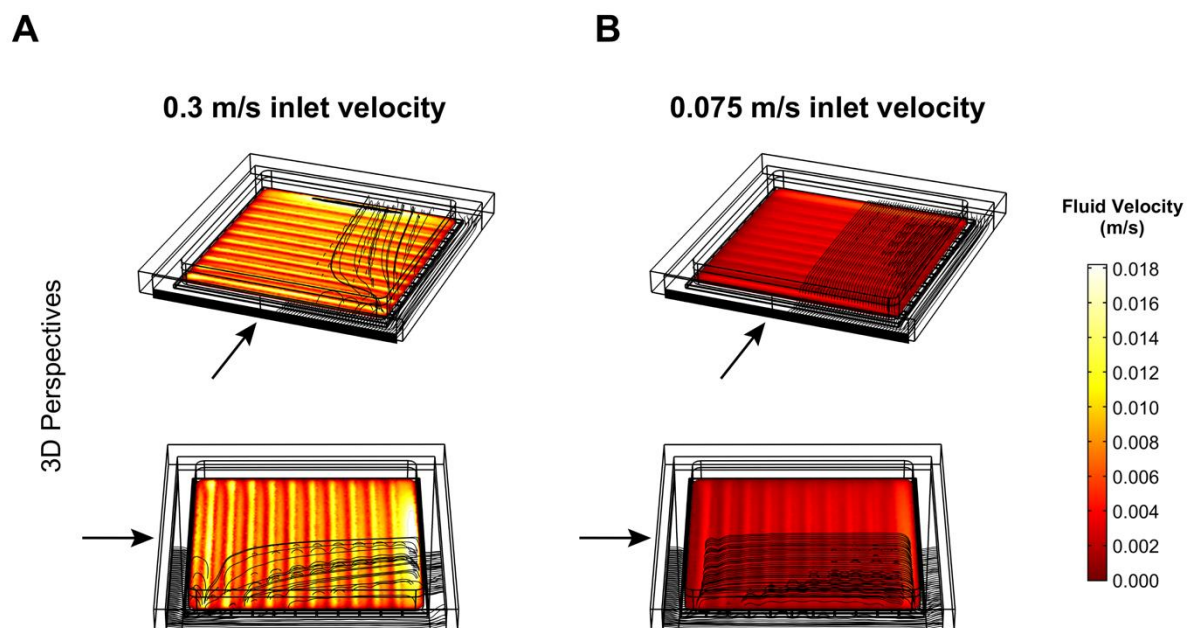
**Supplemental Figure 14.** Normalized cell proliferation data assessed over the course of 6.5 d using a Tox8, resazurin-based metabolic assay. Data plotted are the fluorescent intensity measurements normalized to the initial time point (13.5 h). Aligned vs non-aligned EECMs were not statistically different at any time point.



**Supplemental Figure 15.** CLSM MIP of an aEECM prior to cell seeding (0 d) and approaching cell saturation (4 d), where cells can be observed in the differential interference contrast (DIC) image.



**Supplemental Figure 16.** **A:** induced pluripotent stem cells (iPSCs) seeded onto a fibronectin EECM at a concentration of  $100,000 \text{ cells mL}^{-1}$  (single cell seeding). iPSCs were expanded for 14 d before imaging. **B:** H9 human embryonic stem cell (hESC) colonies seeded on an EECM. Colonies were gathered using a colony picker, transferred in medium and seeded on fibronectin EECMs for 24 h prior to imaging. The yellow outline marks the initial boundaries of the seeded hESC colony. **C:** MDA-MB-231 cells were seeded at  $75,000 \text{ cells mL}^{-1}$  on fibronectin EECMs for 20 h prior to imaging. **D:** SUM-159 cells on an EECM. Fibronectin EECM scaffolds were placed in cell suspension ( $4.0 \times 10^6 \text{ cells mL}^{-1}$ ) for 4 hours before being removed, rinsed with DPBS and imaged. All scale bars =  $100 \mu\text{m}$ .



**Supplemental Figure 17.** Fluid flow characteristics across perpendicularly oriented TPSs at different inlet velocities.